Lithium Batteries

DOI: 10.1002/anie.201204591

Nano-Structured Phosphorus Composite as High-Capacity Anode Materials for Lithium Batteries**

Li Wang, Xiangming He, Jianjun Li, Wenting Sun, Jian Gao, Jianwei Guo, and Changyin Jiang*

High-performance lithium-ion batteries have attracted attention for satisfying the demands of communication, portable electronic devices, electric vehicles and hybrid vehicles. Many attempts have been made over the past decade to increase the energy density of lithium-ion batteries. Graphite ($372\ mA\,h\,g^{-1}$) is presently used as an anode material for lithium-ion batteries, but higher capacity anode materials are being extensively researched.[1–6] Among the many possible alternatives, a lot of work has been devoted to metal oxides,[7,8] Sn-based composites,[9] Si-based composites,[10–12] because of their ability to react reversibly with large amounts of Li per formula unit. Elemental phosphorus is another potentially attractive anode material with a theoretical specific capacity of $2595\ mA\,h\,g^{-1}$, assuming a complete reaction, $3\,Li + P \rightarrow Li_3P$.[6,13,14] Phosphorus has three main allotropes: white, red, and black.[15] Among these allotropes, white phosphorus is chemically unstable. Black phosphorus is thermodynamically the most stable, but the most difficult to synthesize.[6]

Red phosphorus is an abundant and eco-friendly material. However because of its electronic insulation, the experimental capacity of red phosphorus is far from the theory value and dramatically fades after a few cycles.[14,16] Nazar and coworkers reported the benefit of nano-structuring sulfur composite materials with mesoporous carbon molecular sieves as the host material, resulting in improvements of both capacity release and stable cycling.[17] In such a material, the conductive mesoporous carbon framework improves the electrical conductivity of the supported material. Although sulfur is an electronic insulator, the composite shows good performance. These results inspired us to prepare a phosphorus composite. However, it is difficult to fabricate a nano-structured red phosphorus composite, which is essential for improvement of the electrochemical performance of red phosphorus.

Herein, we demonstrate a facile preparation of a nano-structured red phosphorus composite for lithium storage for use as an anode material. Particularly, this composite shows a highly reversible charge/discharge processes, stable cycling, and a high lithium-storage capacity of over $750\ mA\,h\,g^{-1}$, which is based on the composite (porous carbon + phosphorus). Utilization of phosphorus in the composite reaches up to 92% (that is, 92% phosphorus is fully used for reversible lithium storage in the composite), which is equivalent to a capacity of $2413\ mAh\,g^{-1}$ based on red phosphorus.

The phosphorus composite was prepared by a vaporization/adsorption strategy. Porous carbon powder and red phosphorus powder were placed separately in a vessel which was then sealed (see Scheme 1). The vessel was filled with pure argon. Then the vessel was then heated to just above the sublimation temperature of red phosphorus. The sublimate diffused into the pores by capillary forces and pressure differences, whereupon it was adsorbed and deposited on the internal surface of the porous carbon.

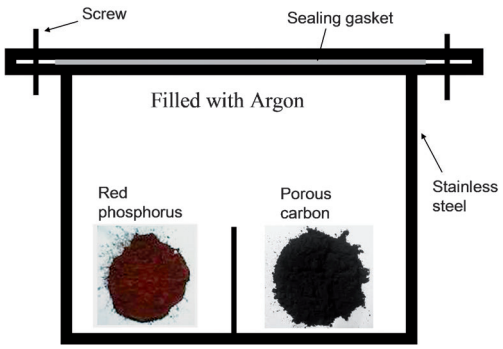

Scheme 1. Apparatus for the preparation of red phosphorus/carbon composite.

The weight analysis of sample gives 30.56 wt.% phosphorus content in the composite (see Supporting Information). The BET surface area and BJH porous volume of starting materials and the composite are given in Table 1. Red phosphorus is a non-porous powder mainly consisting in bulky grains, while porous carbon shows a high surface area ($917\ m^2\,g^{-1}$) and a large porous volume ($0.186\ cm^3\,g^{-1}$). After adsorption of phosphorus, the surface area and porous volume dramatically decrease to $2.9\ m^2\,g^{-1}$ and $0.025\ cm^3\,g^{-1}$, respectively. This result indicates that the pores in the carbon

[*] Dr. L. Wang, Dr. X. M. He, Dr. J. J. Li, W. T. Sun, Dr. J. Gao, Dr. J. W. Guo, Prof. C. Y. Jiang
Institute of Nuclear and New Energy Technology
Tsinghua University
Beijing, 100084 (P.R. China)
E-mail: hexm@tsinghua.edu.cn
Dr. X. M. He
State Key Laboratory of Automotive Safety and Energy
Beijing, 100084 (P.R. China)
Dr. J. J. Li
Beijing Key Laboratory of Fine Ceramics
Beijing, 100084 (P.R. China)

[**] We gratefully thank the National Natural Science Foundation of China (No. 20901046), the Ministry of Science and Technology (No. 2011CB935902 and No. 2010DFA72760) and the Tsinghua University Initiative Scientific Research Program (No. 2010THZ08116, No.2011THZ08139 and No. 2011THZ01004).

Supporting information for this article is available on the WWW under http://dx.doi.org/10.1002/anie.201204591.

Table 1: BET surface area of the composite, phosphorus, and porous carbon

Parameter	Phosphorus powder	Porous carbon	composite
BET Surface area [$m^2 g^{-1}$]	2.46	917	2.9
BJH Pore volume [$cm^{-3} g^{-1}$]	0.009	0.186	0.025

are mostly filled by the deposited phosphorus, as further confirmed by N_2 adsorption–desorption isotherms and the pore size distribution of the porous carbon and the composite (see Figure S1 in the Supporting Information). In addition, based on the pore volume of carbon (0.186 $cm^3 g^{-1}$) and the density of red phosphorus (2.2 $g cm^{-3}$), the content of phosphorus in the "filled" carbon is about 29.04 wt%. Considering of phosphorus deposition on external surface of carbon particles, the measured phosphorus content (30.56 wt%) is reasonable.

Thermogravimetric (TG, Netzsch STA 409 PC) analysis of phosphorus composite (Supporting Information, Figure S2) shows a slight weight loss at about 500 °C under an argon atmosphere, whereas red phosphorus shows a sharp weight loss at about 410 °C the temperature at which red phosphorus sublimes, indicating that phosphorus in the composite is more stable than elemental phosphorus, resulting from the adsorption of phosphorus on the surface of carbon. Under an air atmosphere, thermogravimetric analysis of the phosphorus composite (Figure S3) shows a slight weight loss at 150 °C, probably loss of adsorbate, followed by a slight weight gain and small exothermic peak at 200 °C, resulting from oxidation. The phosphorus composite also shows a slight weight loss after 400 °C under air atmosphere, whereas red phosphorus alone shows a weight gain at about 410 °C corresponding to the red phosphorus being oxidized. The red phosphorus then shows a sharp weight loss and sharp exothermic peak at 515 °C, corresponding to the red phosphorus catching fire. These results also indicate that the phosphorus in the composite is more stable than elemental red phosphorus in the air. Furthermore, an ignition test carried out with a cigarette lighter, shows that the composite cannot be ignited, whereas the elemental red phosphorus is ignited and burn (see video in Supporting Information). Again these results demonstrate that the adsorption of phosphorus by porous carbon makes it chemically stable in the air. Therefore, the thermal stability of the composite is expected to be sufficient for battery applications.

The TEM image clearly shows 5–10 nm particles in the composite, as shown in Figure 1a. The SEM image also clearly shows that a small quantity of tiny red phosphorus particles is present on the external surface of a composite particle (Figure 1b). However, the carbon and phosphorus elemental mapping images (Figure 1c,d) clearly demonstrate that the most of phosphorus is homogeneously distributed in the framework of the porous carbon, while a little on the external surface.

The Raman spectrum of porous carbon exhibits characteristic G- and D-bands while the spectrum of red phosphorus shows several well defined peaks in the 300–500 cm^{-1} region

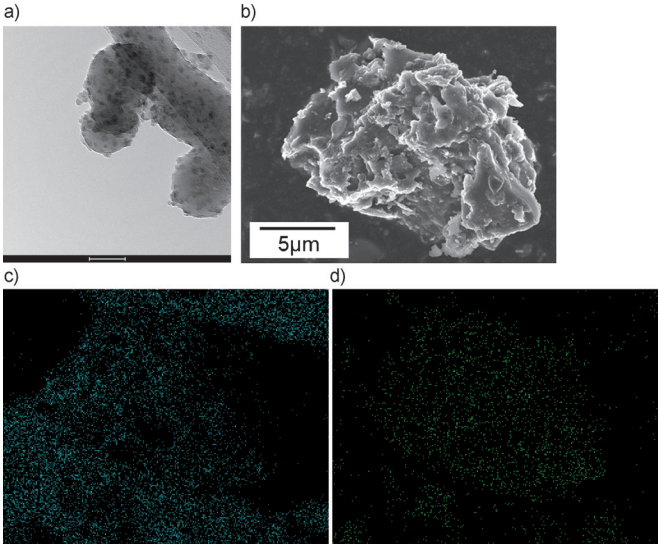

Figure 1. a) TEM image of the phosphorus/porous carbon composite; scale bar: 50 nm. b) SEM image. c) Carbon and d) and phosphorus elemental mapping images showing the homogeneous distribution of phosphorus in the porous carbon particle.

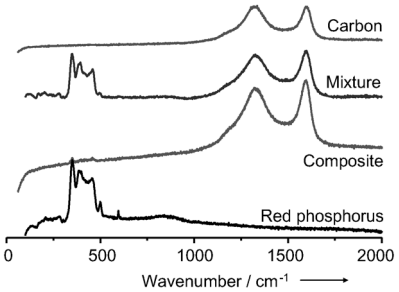

Figure 2. Raman spectra of carbon, red phosphorus, a mixture of carbon and phosphorus, and the phosphorus/porous carbon composite.

(Figure 2). The G mode of graphite (ca. 1580 cm^{-1}) involves an E_{2g} symmetrical bond stretching motion of pairs of C sp^2 atoms, while the D band (ca. 1350 cm^{-1}) is attributed to the breathing mode of six-membered rings.[18] The Raman intensity and wavenumber of both D- and G-bands are unchanged in the spectra of the composites, indicating that the carbon matrix and the adsorbed phosphorus have no interaction in the composite materials. However, the bands arising from phosphorus almost disappear, only a trace can be observed. This trace, evident in the range 320–490 cm^{-1}, confirms the presence of elemental phosphorus in the composite. Amorphous red phosphorus consists of P_7 and P_9 cages arranged to form pentagonal tubes in paired layers; P_9 cages are considered responsible for the sharp peak at approximately 350 cm^{-1}.[18] This signal indicates that amorphous phosphorus is physically adsorbed in the carbon matrix. The X-ray diffraction indicates that the pattern from phosphorus near 15° disappears in the composite, but the diffraction pattern of carbon remains (Figure S4). This result strongly supports the conclusions drawn from the Raman spectra.

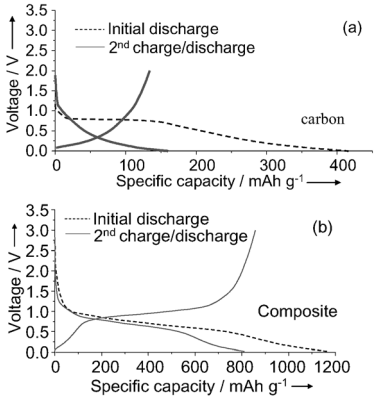

Figure 3. Charge–discharge profiles of the initial two cycles at a current density of 100 mA g^{-1} a) carbon, b) phosphorus/porous carbon composite (30.56% phosphorus).

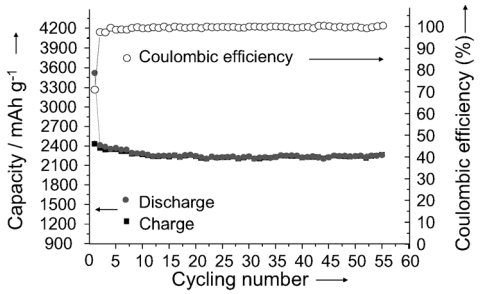

Figure 4. Cycle performance of the phosphorus/porous carbon composite in the electrolyte of 1 M $LiPF_6$/EC + DMC + EMC. The capacity is referred to the effective composite material.

Figure 3 shows charge/discharge curves of the matrix carbon and the composite at the initial discharge process and the second cycle process. During the first discharge, carbon delivers the first discharge capacity of 416 mAh g^{-1}, and presents cycling capacities of about 150 mAh g^{-1} in the following cycles. A composite/Li cell was assembled and tested for its electrochemical behavior at the current density of 100 mA g^{-1} composite. During the first discharge down to 0 V, the discharge voltage curve shows the insertion of 1200 mAh of lithium ion per gram composite in two processes at 0.75 V and 0.25 V. Upon recharge, up to 3.0 V, 840 mAh of lithium ion can be removed out, leading to an initial coulombic efficiency of 70% and initial irreversible capacity of 360 mAh g^{-1}. Such a large initial irreversible capacity may lead to lithium consumption and reduce the capacity of a real full lithium-ion battery. This situation is a weak point of the composite and needed to be further improved. Fortunately, one of the effective ways to overcome this weak point is to reduce such a large initial irreversible capacity which can be done by lithium compensation.[19,20] Upon cycling, a 745 mAh g^{-1} capacity is retained after 50 charge–discharge cycles. After adsorption of phosphorus, the charge/discharge characteristics of carbon disappear. The composite shows novel charge/discharge characteristics. Phosphorus adsorbed in porous carbon provides a capacity of 2413 mAh g^{-1} phosphorus for reversible lithium storage. 92.85% of phosphorus in the composite is utilized during cycling, a value that indicates the effectiveness of proposed adsorption preparation.

Figure 4 shows the cycle performance of the phosphorus composite between 3.0 V and 0 V in the electrolyte of 1M $LiPF_6$/EC (ethylene carbonate) + DMC (dimethyl carbonate) + EMC (ethylene methyl carbonate). The composite presents an initial coulombic efficiency of 70%, then cycles at the efficiencies over 99.5%, resulting in a good cycling performance. The phosphorus composite shows the capacity retention over 87% from the second cycle to 55th cycle. The average capacity degradation rate is less than 0.2% per cycle excluding the first discharge process. It is of note that the coulombic efficiency (CE) of the phosphorus composite is much improved compared to that of pristine porous carbon (Figure S5). That is, for the composite, the initial CE is 70%, and then CE increases to 99.6% after three cycles. This result is important for practical applications in lithium-ion batteries. The reason is as follows. During cycling, the formation and repair of solid electrolyte interphase (SEI) consumes Li^+ and e^- at the anode, leading to low CE. The lithium-ion cells used in the experiments were flooded with significant amounts of excess electrolyte and lithium foil anode, so that electrolyte and lithium consumption could occur without capacity loss. In a practical lithium-ion cell with a limited amount of electrolyte and lithium, electrolyte and lithium consumption leads to eventual and catastrophic capacity loss. A lower CE implies much greater consumption of electrolyte and lithium which will have an impact on the cycle life for full lithium-ion batteries.[21] Porous carbon has a large surface area which leads to a large solid electrolyte interphase (SEI) area. This in turn leads to low CE during cycling (Figure S5). The initial CE is only 32%, and then CE increases gradually to 98% after 50 cycles. These low CEs imply too much consumption of electrolyte and lithium every cycle. However, after adsorption of phosphorus, the composite has a high CE values of over 99.6% after three cycles (Figure 4) implying less consumption of electrolyte and lithium, leading to better cycle life. Therefore, the phosphorus composite is a potential candidate anode material for lithium-ion batteries. On the other hand, in comparison with spinel $Li_4Ti_5O_{12}$, a material which is also a candidate anode material with promising CE, the voltage of the phosphorus composite is 0.5 V lower than the spinel, and the capacity is five times greater than the spinel, showing that the phosphorus-composite-based battery can store much more energy than the spinel based one in a specific weight. The C-rate performance of the composite was tested, showing good rate capability (Figure S6) again indicating that the phosphorus composite is a promising alternative anode material for lithium-ion batteries.

In summary, we have proposed a simple method to synthesize a nano-structured phosphorus composite material from porous carbon and red phosphorus, in which the porous carbon serves as the electronically conductive support matrix. Nanomaterials are normally of high surface area, which is a disadvantage for anode materials because a large surface area can lead to low coulombic efficiencies and to unstable cycle performance. This nano-structured phosphorus composite has a low surface area, leading to high coulombic efficiencies, which is important for anode materials. The

phosphorus composite exhibits highly reversible charge/discharge processes with high utilization of phosphorus. The composite shows a reversible capacity of up to 800 $mA\,h\,g^{-1}$ at 100 $mA\,g^{-1}$, and a stable cycle performance with high coulombic efficiencies. In view of its high capacity of lithium storage, the phosphorus composite has promise for applications in electrochemical energy storage devices with high energy density. The results also give clear evidence of the utility of porous carbon to enhance the electrochemical performance of red phosphorus as an anode material for lithium-ion batteries with high energy density. This preparation strategy is simple, yet very effective, and because of its versatility, could potentially be extended to other electrically conductive supporting matrices (e.g. graphene) for the preparation of other phosphorus composites for lithium-ion batteries.

Experimental Section

Red phosphorus was washed with distilled water to remove oxides before processing. Red phosphorus (10 g) was put on the bottom of the stainless steel vessel and porous carbon (2 g) was put into a small beaker which was placed into the same stainless steel vessel. The vessel was sealed in an argon-filled glove box. Then the vessel was heated at 450 °C for 3 h. 2.88 g of composite material was obtained. The content of phosphorus in composite was analyzed to be 30.56 %.

Received: June 13, 2012
Published online: August 2, 2012

Keywords: anode materials · electrochemistry · lithium battery · nanostructure · phosphorus

[1] A. S. Aricò, P. Bruce, B. Scrosati, J. M. Tarascon, W. Van Schalkwijk, *Nat. Mater.* **2005**, *4*, 366 – 377.
[2] J. Maier, *Nat. Mater.* **2005**, *4*, 805 – 815.
[3] V. Etacheri, R. Marom, R. Elazari, G. Salitra, D. Aurbach, *Energy Environ. Sci.* **2011**, *4*, 3243 – 3262.
[4] P. G. Bruce, B. Scrosati, J. M. Tarascon, *Angew. Chem.* **2008**, *120*, 2972 – 2989; *Angew. Chem. Int. Ed.* **2008**, *47*, 2930 – 2946.
[5] C. X. Zu, H. Li, *Energy Environ. Sci.* **2011**, *4*, 2614 – 2624.
[6] C. M. Park, H. J. Sohn, *Adv. Mater.* **2007**, *19*, 2465 – 2468.
[7] P. Poizot, S. Laruelle, S. Grugeon, L. Dupont, J. M. Tarascon, *Nature* **2000**, *407*, 496 – 499.
[8] S. Fang, Y. Tang, X. Tai, L. Yang, K. Tachibana, K. Kamijima, *J. Power Sources* **2011**, *196*, 1433 – 1441.
[9] Y. Idota, T. Kubota, A. Matsufuji, Y. Maekawa, T. Miyasaka, *Science* **1997**, *276*, 1395 – 1397.
[10] Z. S. Wen, J. Yang, B. F. Wang, K. Wang, Y. Liu, *Electrochem. Commun.* **2003**, *5*, 165 – 168.
[11] Y. Cui, Z. Zhong, D. Wang, W. U. Wang, C. M. Lieber, *Nano Lett.* **2003**, *3*, 149 – 152.
[12] L. F. Cui, Y. Yang, C. M. Hsu, Y. Cui, *Nano Lett.* **2009**, *9*, 3370 – 3374.
[13] L. Wang, X. M. He, J. G. Ren, W. H. Pu, J. J. Li, J. Gao, United States Patent Application Publication, US20100239905, **2010**.
[14] C. Marino, A. Debenedetti, B. Fraisse, F. Favier, L. Monconduit, *Electrochem. Commun.* **2011**, *13*, 346 – 349.
[15] D. E. C. Corbridge, *Phosphorus: An Outline of its Chemistry, Biochemistry and Technology, 5th ed.*, Elsevier, Amsterdam **1995**.
[16] S. Boyanov PhD Thesis, Université de Montpellier, **2008**.
[17] X. Ji, K. T. Lee, L. F. Nazar, *Nat. Mater.* **2009**, *8*, 500 – 506.
[18] G. M. Fuge, P. W. May, K. N. Rosser, S. R. J. Pearce, M. N. R. Ashfold, *Diamond Relat. Mater.* **2004**, *13*, 1442 – 1448.
[19] C. R. Jarvis, M. J. Lain, M. V. Yakovleva, Y. Gao, *J. Power Sources* **2006**, *162*, 800 – 802.
[20] H. Sun, X. M. He, J. G. Ren, J. J. Li, C. Y. Jiang, C. R. Wan, *Electrochim. Acta* **2007**, *52*, 4312 – 4316.
[21] A. J. Smith, J. C. Burns, S. Trussler, J. R. Dahn, *J. Electrochem. Soc.* **2010**, *157*, A196 – A202.

